

EXPERIMENTAL RESULTS ON THE RADIO REMOTE CONTROL AND REMOTE MONITORING OF THE ANTI-HAIL MISSILE LAUNCHPADS

Sorin STEPAN¹, Gheorghe MANOLEA²

¹Conestoga College, Ontario, Canada

²University of Craiova, Romania

sostepan@yahoo.com¹, ghmanolea@gmail.com²

Summary. The paper presents a technical solution for monitoring and operating the anti-hail missile launchpads using an internet-connected wireless remote control, which operates in the 433 MHz ISM frequency band. A small size experimental model of the real launchpad was devised and built, in order to test the local operation of the remote control and its over-the-internet monitoring function. When designing the experimental model, attention was given to preserving the characteristics of the actual launchpad, such that after testing the technical solutions of the remote control on the model, they could be implemented on the real launchpad with minimal modifications. This experimental model can also be used for staff training during the active off-season. The proposed technical solution presents an example of how the electrical machine, seen as an element of execution, is included in the concept of the Internet of Things.

1. INTRODUCTION

The anti-hail system in Romania was created under the Government decision HG no.604 of July 28, 1999, regarding the approval of the Program for the implementation and financing of the National anti-hail System and has been systematically developed. The implementation of this system is done through the Government's annual decisions. First, the organizational structure of the Prahova Territorial Unit was checked, and the basic components of both the anti-hail missile and the missile launchpad were made. Then, through internal research such as Ph.D. theses and contract research, these basic components were developed and modernized. Any additional complementary equipment useful for active interventions in the atmosphere was added.

The experimental model of the anti-hail missile launchpads was designed to verify the technical solutions for the remote control, operated locally or from the Command Center located at 50-80km [1].

2. THE REMOTE CONTROL

2.1 Making the remote control

The radio remote control is built with two ASD-DTU-100 transceivers that use LoRa modulation. They provide the radio link between a touch screen used by the operator and a PLC controller connected to the launchpad, using a frequency in the 433 MHz ISM band (fig. 1) [7], [8].

The commands entered by the operator are grouped into three pages on the touch screen: manual positioning, automatic positioning, and the list of events. Positioning the launchpad from the automatic positioning screen, and launching the missiles are considered as events. All the events are recorded on an external SD card or a USB flash, which is attached to

the remote control. In parallel with the touch screen, the launchpadpositioning and the missile launching commands can be sent from a local control panel, connected by cables to the PLC controller. The remote control has an Ethernet port, which makes the remote monitoring and control of the launchpad possible when using a computer connected to the Internet. Access to the remote control is password protected and can be disabled by the local operator.

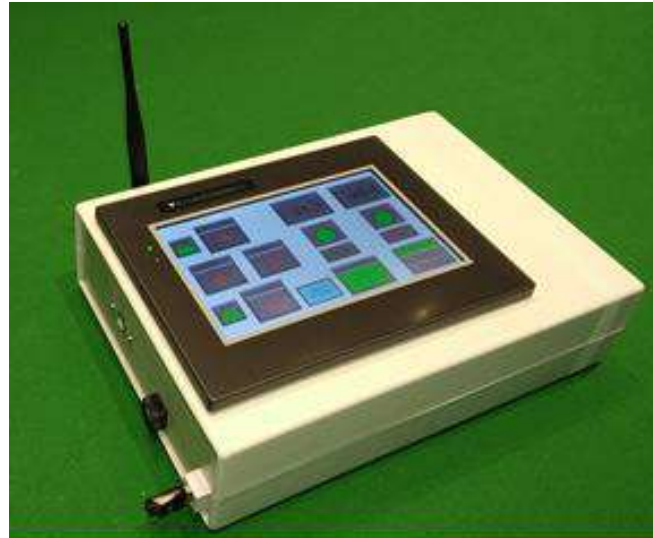


Fig. 1. The remote control

2.2RF measurements

A field test was performed in an urban environment, to measure the operating range of the radio remote control. Power was provided from the internal battery, and the transmitter's power was set to 11 dBm (12.59 mW). The remote control functioned correctly for up to 90 m, after which the radio signal was lost due to attenuation and a loss of the direct line of sight. The radio link was resumed at 60m.

The frequency spectrum and the transmitter output power measurements were performed on a test bench using an Agilent N9010A signal analyzer. The remote control was connected to the signal analyzer through a ZFRSC-42-S+ Rf splitter [10] and two radiofrequency cables provided with SMA connectors.

The transmitter maximum output power and frequency spectrum measurements were performed using the Trace – Max Hold function of the Agilent N9010A tester (fig. 2).

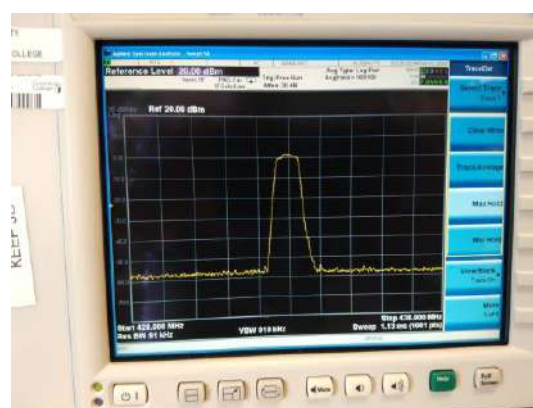


Fig. 2. The transmitter maximum power and frequency spectrum measurements using Trace – Max Hold function of the tester.

A maximum of 2 dBm transmitter output power was measured, which confirms the maximum power of 11 dBm set for the transmitter, considering the RF splitter attenuation of 6 dB and the power loss on cables and connectors of about 3 dB.

LoRa type modulation is well known for the very low average transmitted power, due to the 1% or less on-air duty cycle, limited by regulations. Figure 3 shows the result of the frequency spectrum and the average transmitter output power measurements, using the Trace – Average function of the Agilent N9010A tester for the same transmitter settings as in maximum output power measurements presented in figure 2.

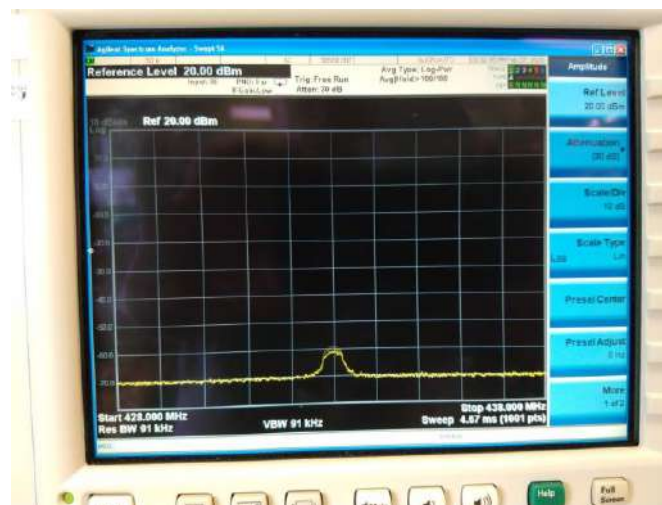


Fig. 3. The frequency spectrum and the average transmitter output power measured with the Agilent N9010A tester using the Trace – Average function.

It can be seen from figures 2 and 3 that the level of the radiated power outside the 1 MHz RF channel is 30 dB lower than the maximum power, which means that 99.9% of the power is radiated inside the chosen frequency channel. This proves the high spectral efficiency and adjacent channel power performance of the transmitter.

The very low measured average transmitter output power is not at all surprising. LoRa-type modulation and LoRaWAN communication protocol have been specifically created for low-volume data communications between isolated, battery-powered sensors and internet-connected network nodes, where energy saving is a priority.

3. THE EXPERIMENTAL MODEL OF THE LAUNCH RAMP

3.1 The mechanical structure of the experimental model

The experimental model, shown in the figures (4.-6.), reproduces the positioning function of the actual launch pad on azimuth and elevation and simulates the launching of two missiles [2], [9].

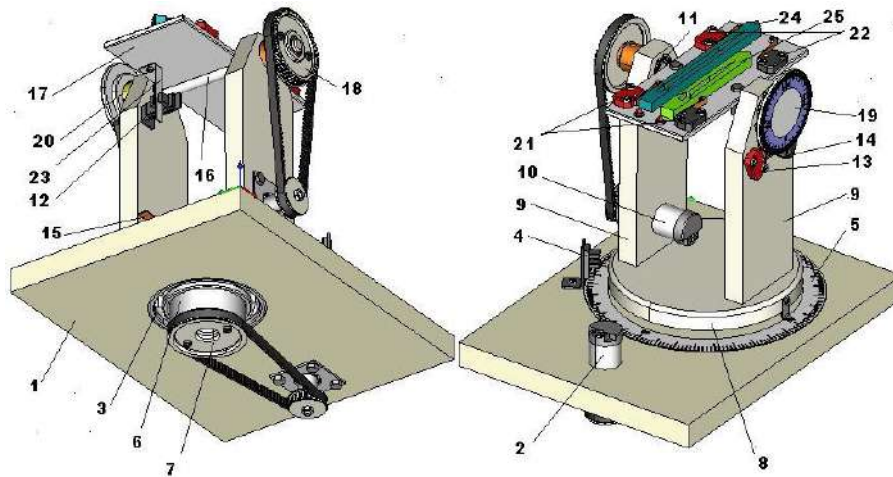


Fig. 4. The experimental model drawing

The figure 4 legend is illustrated in table 1.

Tab.2. Figure 4 legend

Reference number	Explanation
1	Base plate, 338 x 257 x 25 mm, Delrin
2	DC motor, azimuth (SPG30E-270K)
3	Bearing, azimuth (110 x 70 x 20 mm)
4	Home position sensor, azimuth (Omron EE-SX460-P12)
5	Circular scale, azimuth
6	Cylindrical shaft, Delrin, L=55 mm, D=70 mm, azimuth
7	Timing pulley, 40 teeth, 57105K28, azimuth
8	Rotating plate, azimuth, D=180 mm, H=18 mm, Delrin
9	Vertical walls, Delrin
10	DC motor, elevation (SPG30E-270K)
11	Bearings, elevation (30 x 10 x 8 mm)
12	Home position sensor, elevation (Omron EE-SX460-P12)
13	Limit switch, elevation 20°
14	Limit switch, elevation 85°
15	Cable clamp
16	Shaft, L=160 mm, D=10 mm, elevation
17	Missiles plate, 204 x 80 x 6 mm, Plexiglas acrylic
18	Timing pulley, 40 teeth, 57105K28, elevation
19	Circular scale, elevation
20	Cam, elevation, for 20° and 85° limit switches
21	Microswitch, detects missile presence
22	Microswitch, detects missile type
23	Home position sensor mobile element, elevation
24	Long missile
25	Short missile

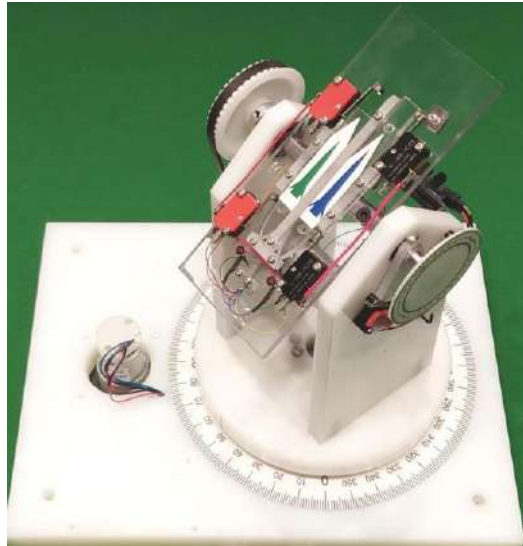


Fig.5.The experimental model ofthelaunchpad

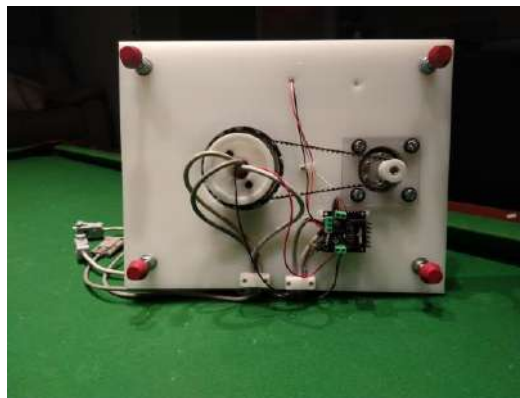


Fig.6. The experimental model -bottom view

3.2 Choosing the electrical components of the experimental model

Two SPG30E-270K DCgeared motors were used for the positioning of the experimental model (fig. 7).



Fig. 7. SPG30E-270K DC motor used for azimuth and elevation positioning

The transmission ratio of the motor gears is 1:270. An external 1:4 gears and timing belt transmission is present in both the azimuth and elevation directions.

The DC motors have 1.1 W of power, at 12V nominal voltage[3].

The quadrature encoders on the motors require 5V DC power and provide 7 pulses per revolution.

Considering:

$N_1 = 270$ the transmission ratio of the motor gears,

$N_2 = 4$ the transmission ratio of the gears and belt,

$N_3 = 7$ pulses per revolution at the motor shaft

The number N of pulses provided by the encoders for one-degree rotation of the launchpad on either of the two axes – azimuth or elevation - can be calculated (1):

$$N = \frac{N_1 N_2 N_3}{360} = 21 \quad (1)$$

The pulses on both the A and B encoder channels are counted by the PLC while the launchpad is moving, and the number N determines the maximum accuracy of the positioning, which is theoretically 1/84 degrees (fig.8). The positioning accuracy is lower due to the mechanical play in the bearings and the elasticity of the transmission belts.

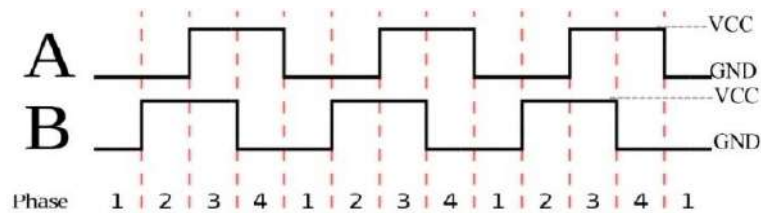


Fig. 8. The quadrature encoder output pulses

Although the DC motors have a nominal voltage of 12V, they were powered with 5V, to reduce the rpm. The decreased power does not affect the normal operation of the experimental model. Thus, the model executes a full rotation in about 55 seconds.

The driver module used to control the two DC motors is presented in fig.9 [4].

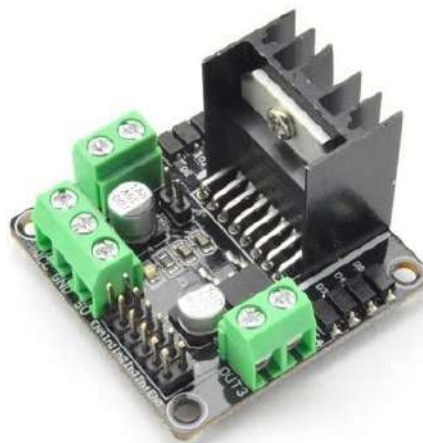


Fig. 9. The driver module used to control the two DC motors

The driver module, based on the L298N integrated circuit, can drive a step-by-step motor or two DC motors, as in this application.

The driver module's electronic schematic is shown in fig. 10 [5].

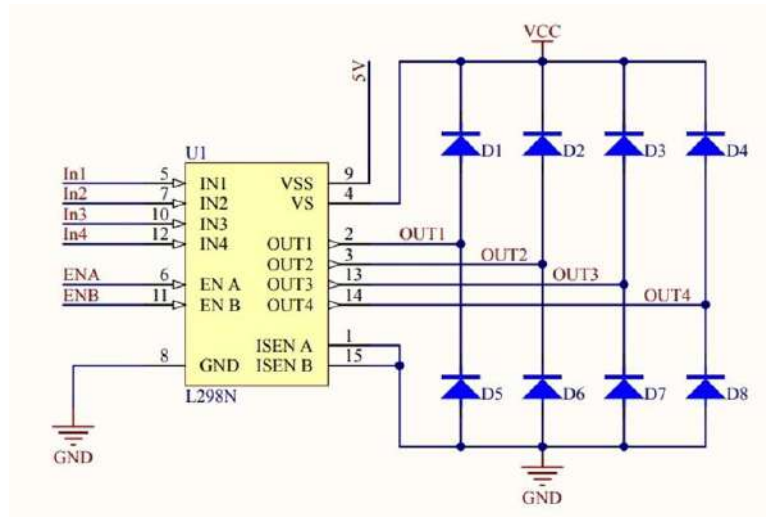


Fig. 10. Electronic schematic of the driver module

The integrated circuit L298N contains a dual bridge with transistors and can drive inductive loads, such as step-by-step motors or DC motors, at a voltage of up to 46V and a total maximum current of 4 A [6].

The choice of the DC motors and the driver module when designing the experimental model was not randomly taken. The two DC motors connect to the OUT1-OUT2 and OUT3-OUT4 driver outputs. The control inputs for the driver module are IN1, IN2, and ENA for the azimuth motor, and IN3, IN4, and ENB for the elevation motor. The control of the two DC motors is similar to that of the AC motors on the actual launchpad, where each motor is driven by an intelligent AC drive, with the FWD, REV, and ENABLE control inputs. Only the voltage levels are different: the driver module on the experimental model works with 5V signals, and the AC drives control inputs accept 24V signals.

The logic used by the driver module is illustrated in tables 2 and 3.

Tab.2. The logic commands for the azimuth motor

IN1	IN2	Ena	Azimuth motor
X	X	0	Stop
0	0	X	Stop
1	0	1	Rotate to the right
0	1	1	Rotate to the left

Tab.3. The logic commands for the elevation motor

IN3	IN4	ENB	Elevation motor
X	X	0	Stop

0	0	X	Stop
1	0	1	Increase elevation
0	1	1	Decrease elevation

The electrical diagram of the experimental model is presented in fig.11.

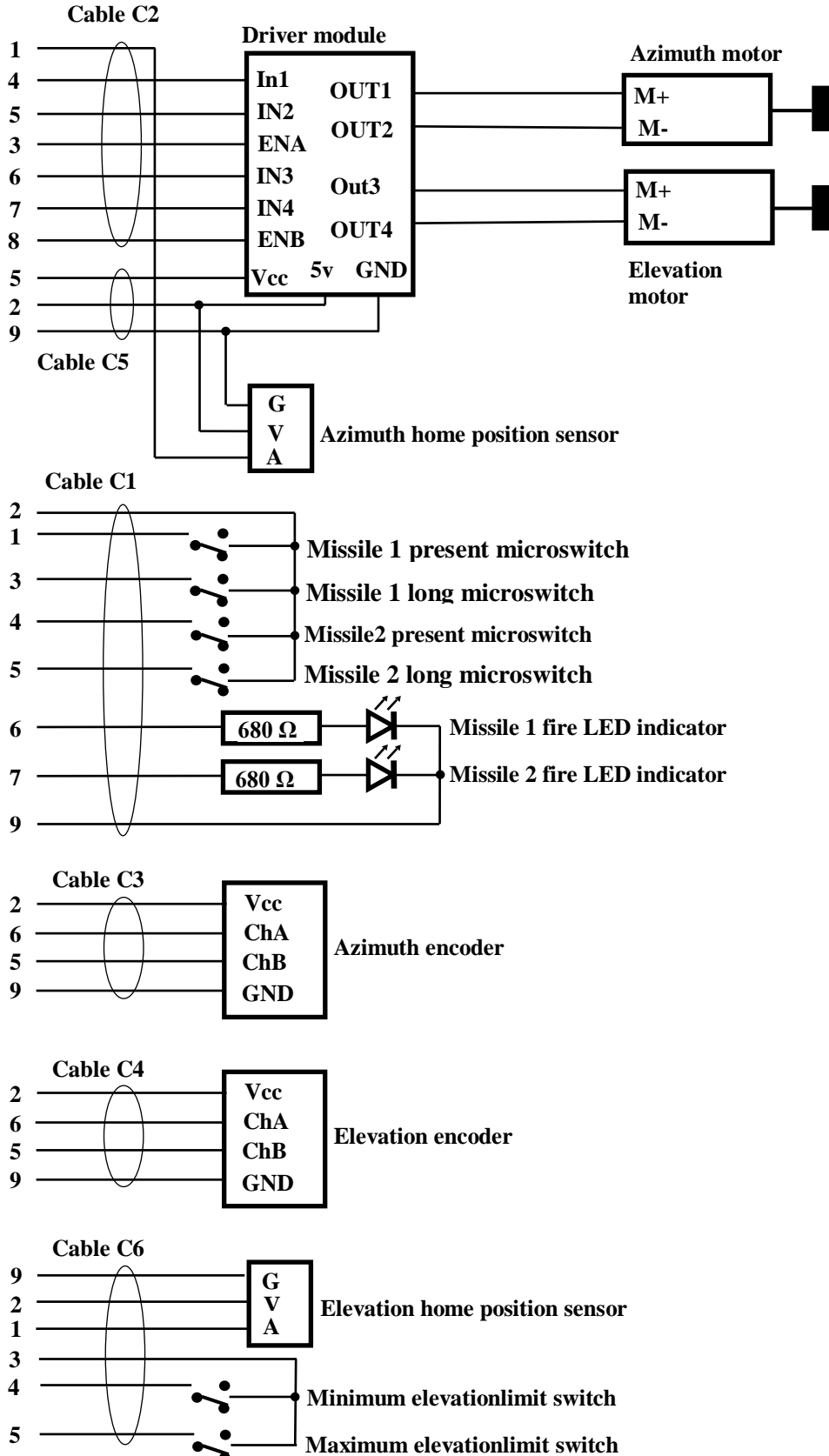


Fig. 11. Electrical diagram of the experimental model of the launchpad

4. MONITORING THE MISSILES LAUNCHPAD IN THE COMMAND CENTRE

To remotely connect to the touch screen using an internet-connected computer, a supervisor in the Command Centre only needs: the IP address of the router to which the touch screen is connected, the account name and the password. An internet browser must be used, and no additional software is required. Another option is to use an iPhone or iPad tablet, in which case the C-more Remote HMI free app must be installed.

To monitor the launchpad in the Command Centre, the following settings must be performed on the remote control and the router:

- Set the same static LAN IP address for the touchscreen and PLC. The Default Gateway setting is the router's LAN IP address, usually 192.168.0.1 or 192.168.1.1, depending on the router type.
- Set the DNS server address to the address being taken from the router configuration.
- Enable the Web Server application on the C-more program loaded on the touchscreen.
- Select port 80 for the Web Server app.
- Enable the Remote Access application on the C-more program loaded on the touch screen.
- Select port 11102 for the Remote Access app (fig. 12).
- Open ports 80 and 11102 from the Port Forwarding menu of the router to which the touchscreen is connected (fig. 13).
- Specify the router WAN IP Address in the Remote Connection tab on the Remote Access app.
- Set the user accounts View, View & Screen Change, and Full Control in the Remote Access app, with or without setting a password.

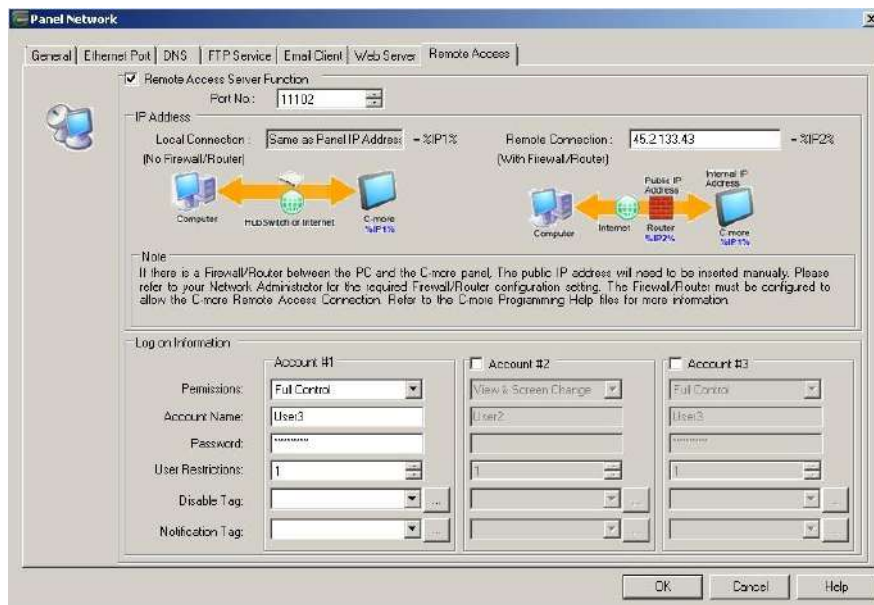


Fig. 12. Remote Access app settings

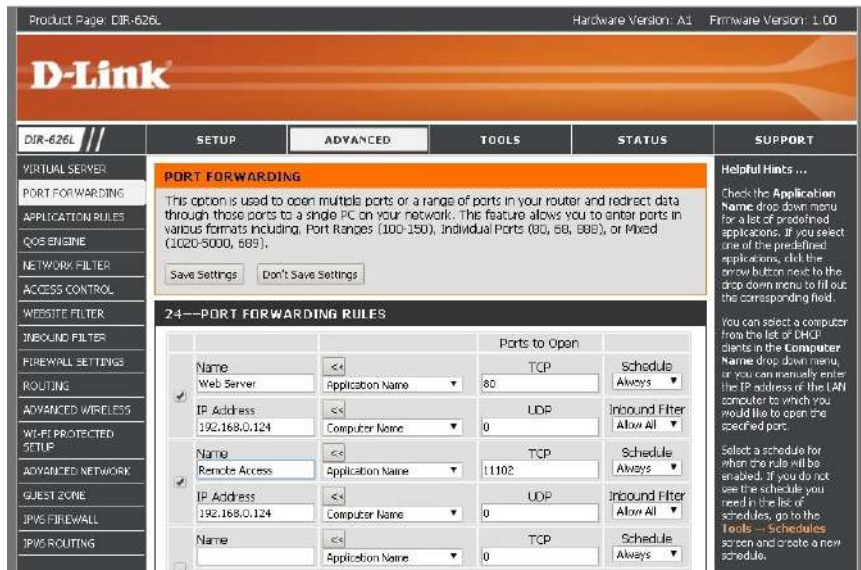


Fig. 13. Port Forwarding router menu settings

5. CONCLUSIONS

The experimental model of the anti-hail missile launchpad presented in this paper was designed and built for the purpose of testing the prototype of a remote control for the launchpad.

During the designing and building process of the launchpad experimental model and the remote control, the authors took the mechanical and electrical characteristics of the actual launchpad into account. The remote control can be easily implemented in the production of the actual launchpad with minimal modifications, and the experimental model can be used to train the operator personnel in the Anti-hail System.

The paper presented here is an example of how the electrical machine, seen as an element of execution, is included in the concept of the Internet of Things.

Acknowledgment

The radio remote control and the experimental model of the launchpad were designed and built as part of the doctoral research carried out by the first author.

Authors' contributions

First author – 90%

Second author – 10%

Bibliography

- [1] Manolea, G., Alboteanu, I.L., Şulea, C., Nicolae, M.Ş. et. all, „Echipamente complementare pentru Sistemul anti-grindină din România”, *editura Sitech, 2014, ISBN 978-606-11-4073-2*
- [2] Stepan, S., „Cercetări privind telecomanda radio a sistemelor de poziționare a rampelor de lansare a rachetelor anti-grindină”, *Teză de doctorat, Craiova, 2020*
- [3] <https://www.cytron.io/p-12v-16rpm-14kgfcm-brushed-dc-g geared-motor-with-encoder>
- [4] <https://www.robotshop.com/en/dc-motor-driver-module.html>
- [5] <https://www.robotshop.com/media/files/pdf/dc-motor-driver-module-schematic.pdf>

-
- [6] <https://pdf1.alldatasheet.com/datasheet-pdf/view/22440/STMICROELECTRONICS/L298N.html>
- [7] Stepan, S., Manolea, G., „Wireless remote control for the anti-hail missiles launch ramp positioning system”, *Analele Universității din Craiova*, 2020
- [8] Stepan, S., Manolea, G. „Contributions regarding the monitoring in the Command Center of the anti-hail launch pads”, *Analele Universității din Craiova*, 2020
- [9] Stepan S., Manolea G. Contribuții privind realizarea și experimentarea unui model la scară redusă al rampei de lansare a rachetelor antigrindină. *Simpozionul de mașini electrice SME '20, București*, 2020
- [10] *** <https://www.minicircuits.com/pdfs/ZFRSC-42+.pdf>